geosciences

MDPI

Article

Stable Isotope Evaluation of Geothermal Gases from the Kızıldere and Tekke Hamam Geothermal Fields, Western Anatolia, Turkey

Selin Süer [1,*], Thomas Wiersberg [2,*], Nilgün Güleç [3] and Fausto Grassa [4]

[1] Central Laboratory, Middle East Technical University, 06800 Ankara, Turkey
[2] Helmholtz Centre Potsdam, GFZ German Research Centre for Geosciences, 14473 Potsdam, Germany
[3] Geological Engineering Department, Middle East Technical University, 06800 Ankara, Turkey; nilgun@metu.edu.tr
[4] Istituto Nazionale di Geofisica e Vulcanologia, Sezione di Palermo, 90146 Palermo, Italy; fausto.grassa@ingv.it
* Correspondence: ssuer@metu.edu.tr (S.S.) and wiers@gfz-potsdam.de (T.W.)

Abstract: Volatiles transported from the Earth's interior to the surface through permeable faults provide insights on the gas composition of deep reservoirs, mixing and migration processes, and can also be applied as gas-geothermometer. Here, we present carbon ($\delta^{13}C$), hydrogen ($\delta^{2}H$) and nitrogen ($\delta^{15}N$) isotopic data of CO_2, CH_4, and N_2 from gas samples collected from the Kızıldere and Tekke Hamam geothermal fields, located along the eastern segment of the Büyük Menderes Graben, Turkey. The stable isotopic composition of carbon ($\delta^{13}C$) ranges from +0.30 to +0.99‰ (PDB) for CO_2 from Kızıldere and is slightly more variable (−0.95 to +1.3‰) in samples from Tekke Hamam. Carbon isotope data in combination with $CO_2/^{3}He$ data reveal that ~97% (Tekke Hamam) to ~99% (Kızıldere) of CO_2 derives from limestone sources, with the residual CO_2 being magmatic in origin with no evidence for CO_2 from organic sources. The slightly higher contribution of limestone-derived CO_2 in Kızıldere, compared to Tekke Hamam can be attributed to the higher temperatures of the Kızıldere reservoir and resulting amplified fluid–limestone interaction, as well as helium depletion during phase separation for Kızıldere samples. In contrast to the carbon isotopic composition of CO_2, the $\delta^{13}C$ values of methane from Kızıldere and Tekke Hamam are clearly distinct and vary between −23.6 and −20.8‰ for Kızıldere and −34.4 and −31.7‰ for Tekke Hamam, respectively. The $\delta^{2}H$-CH_4 composition is also distinct, measured as −126.7‰ for Kızıldere and −143.3‰ for Tekke Hamam. CO_2-CH_4 carbon isotope geothermometry calculations based on the isotopic fractionation of $\delta^{13}C$ between the dominant component CO_2 and the minor component CH_4 reveals temperatures 20–40 °C and 100–160 °C higher than the bottom–hole temperatures measured for Tekke Hamam and Kızıldere, respectively. Based on the CO_2-CH_4 carbon isotope disequilibrium, unusual high methane concentrations of ~0.3 to 0.4 vol.-% and $CH_4/^{3}He$-$\delta^{13}C$-CH_4 relationships we suggest thermal decomposition of late (Tekke Hamam) to over-mature (Kızıldere) organic matter and, to some extent, also abiogenic processes as principal source of methane. The $N_2/^{36}Ar$ ratios of most samples reveal the existence of a non–atmospheric nitrogen component within the gas mixture issuing from both fields, in addition to a constant contribution of atmospheric derived nitrogen accompanied into the system via the meteoric recharge of the geothermal system. Based on the $\delta^{15}N$ isotopic ratios (varying between −4.44‰ and 4.54‰), the non–atmospheric component seems to be a mixture of both sedimentary (crustal organic) and mantle nitrogen. The thick Pliocene sedimentary sequence covering the metamorphic basement is the likely major source for the thermogenic content of CH_4 and crustal N_2 gas content in the samples.

Citation: Süer, S.; Wiersberg, T.; Güleç, N.; Grassa, F. Stable Isotope Evaluation of Geothermal Gases from the Kızıldere and Tekke Hamam Geothermal Fields, Western Anatolia, Turkey. *Geosciences* **2022**, *12*, 452. https://doi.org/10.3390/geosciences12120452

Academic Editors: Gianluca Groppelli and Jesus Martinez-Frias

Received: 16 October 2022
Accepted: 2 December 2022
Published: 9 December 2022

Publisher's Note: MDPI stays neutral with regard to jurisdictional claims in published maps and institutional affiliations.

Keywords: Kızıldere geothermal field; Tekke Hamam geothermal field; source of gas; stable isotopes; thermogenic methane; nitrogen; carbon dioxide

1. Introduction

Stable isotopic evaluation of thermal fluids (water and/or gas), in the form of natural springs, mofettes, and well discharges, has been adopted as a major strategy for the delineation of (i) the possible sources of the fluids (mantle, crust, atmosphere), (ii) the accompanying physicochemical processes affecting the fluids (water-rock interaction, diffusion, isotopic fractionation), (iii) fluid migration along fault zones and the role of faults as conduit or barrier for fluid flow, and (iv) the deep geothermal reservoir temperature conditions within the subsurface. In this regard, several studies have carried out stable isotopic investigations in different geothermal settings throughout the world and presented the effective utilization of carbon ($\delta^{13}C$), nitrogen ($\delta^{15}N$), oxygen ($\delta^{18}O$), and hydrogen ($\delta^{2}H$), in addition to other parameters such as noble gases (e.g., ^{3}He and ^{4}He); gas compositional ratios (CH_4/He, $CO_2/^{3}He$, and N_2/Ar); and water chemistry [1–14].

Kızıldere and Tekke Hamam geothermal fields are two of the most significant high-enthalpy fields located along the eastern segment of the Büyük Menderes Graben in Western Anatolia (Figure 1). The Kızıldere geothermal field, situated along the northern flank of the graben, is a major field supplying fluids for both power generation and direct use applications, such as greenhouse heating, district heating, and CO_2 gas production. The Kızıldere geothermal field currently houses two geothermal power plants: the Kızıldere power plant I in operation since 1984 (total installed capacity: 17.4 Mwe) and the Kızıldere Power plant II in operation since 2013 (installed capacity of 80 Mwe), both owned by the Zorlu Energy Group since the privatization of the field in 2008 [15]. A total of 44 production and reinjection wells have been drilled in the site since 1968, with depths varying between 370 and 2872 m. The reservoir temperatures vary between 155 °C and 245 °C [16,17]. The Tekke Hamam geothermal field, on the other hand, located along the southern flank of the graben, is a site full of gas discharging mofettes, mud pools, and thermal springs, which are mainly used for health tourism facilities [18].

Until now, several studies have concentrated on the geochemical evaluation of the thermal fluids emerging from the Kızıldere and/or Tekke Hamam geothermal sites [17,19–33], in addition to other fields located in the Western Anatolian Province. These studies were mainly concerned with (i) the delineation of the source of the fluids via the adoption of both chemical (major and trace element chemistry) and isotopic (stable and noble gas isotopes) parameters, (ii) the identification of the possible physicochemical processes that alter the pristine fluid composition within the subsurface and during their ascent to the surface, (iii) the real-time monitoring of the gases emerging from the sites and their possible correlations with the ongoing seismicity of the region, and (iv) the estimation of reservoir temperatures via the utilization of both chemical and gas geothermometers. In this study, we present stable isotopic data of CO_2 ($\delta^{13}C$-CO_2) and of two of the minor gas components issuing from Kızıldere and Tekke Hamam: methane and nitrogen ($\delta^{13}C$-CH_4, $\delta^{2}H$-CH_4 and $\delta^{15}N$-N_2), in addition to gas compositional data of the samples, collected during two separate sampling campaigns conducted in November 2007 and August 2008. The aim of this study is to (i) identify possible sources of these gaseous components via the coupled evaluation of ^{13}C–^{2}H-^{15}N isotopic compositions and mixed elemental–nuclide gas ratios (such as $CO_2/^{3}He$, $N_2/^{36}Ar$, $CH_4/^{3}He$, and $CH_4/C_2H_6+C_3H_8$); (ii) estimate the possible reservoir temperature based on isotope geothermometry calculations ($\delta^{13}C$ geothermometry for CO_2-CH_4); and (iii) compare the findings with previous geothermometry estimations and the observed bottom–hole temperatures.

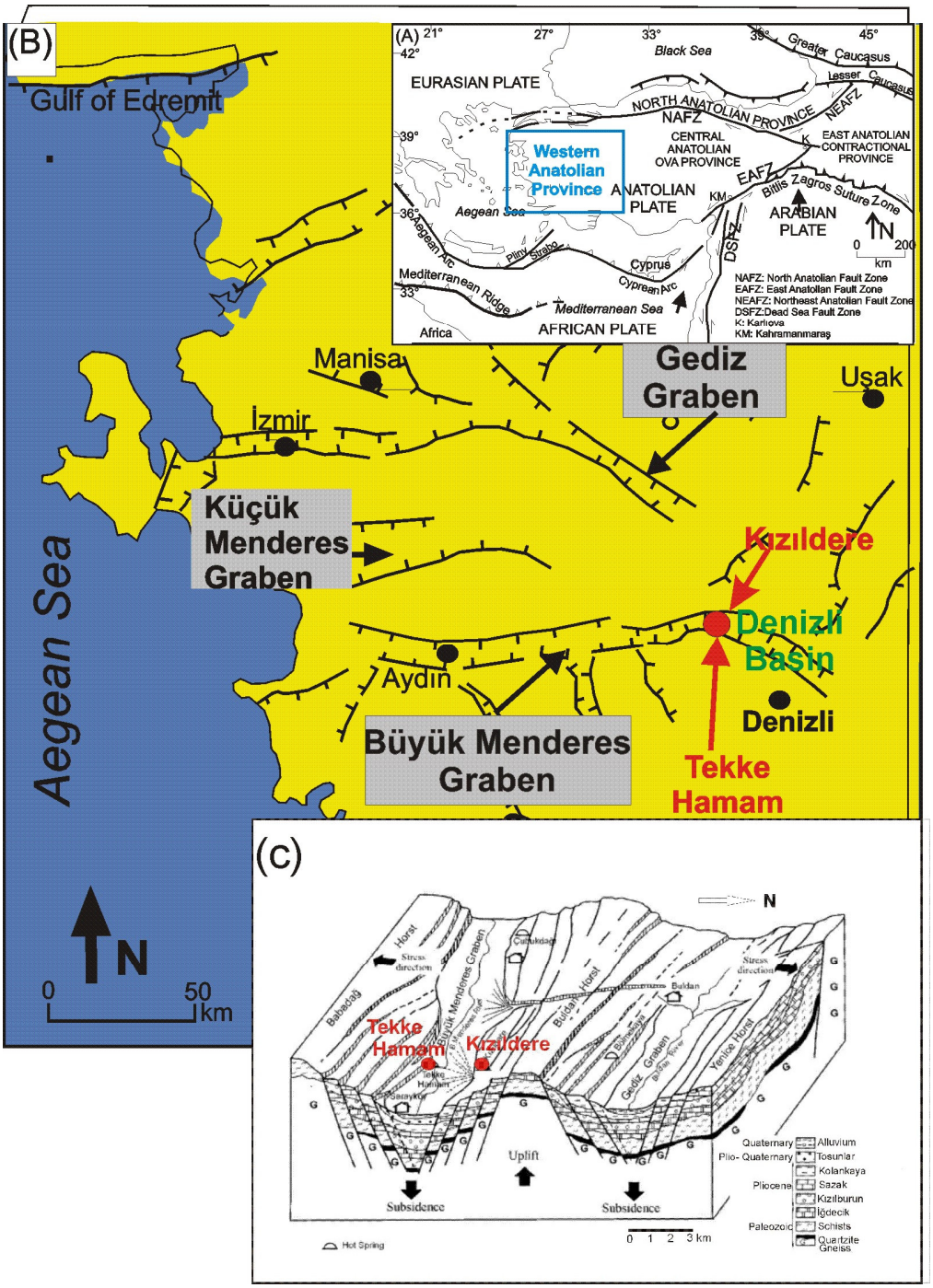

Figure 1. (**A**) Tectonic Map of Turkey, modified from [18], (**B**) simplified map of major structural elements in Western Anatolian Province, including the locations of the Kızıldere and Tekke Hamam geothermal fields, and (**C**) simplified diagram showing the geological framework of the fields, modified from [20].

2. Geological Framework

The Western Anatolian Province (WAP) of Turkey is a region of intense seismic activity that constitutes one of the most important structural features representing the neotectonics period of Turkey [34–36]. Located within the Alpine–Mediterranean belt, the WAP represents a site of horst–graben structures formed in relation to the N–S-directed continental extension prevailing in the region since at least the latest Oligocene–Early Miocene [37]. The high-angle boundary fault network of the horst–graben structures in WAP, in addition to the Neogene–Quaternary volcanism, leads to the widespread oc-

currences of geothermal manifestations, located mostly within moderate to high enthalpy geothermal fields.

This study focuses on two of the most significant geothermal fields situated in the WAP: the Kızıldere and Tekke Hamam high enthalpy geothermal fields, located west of the city of Denizli in the Denizli Basin, which also hosts several other geothermal fields (e.g., Pamukkale, Yenice, Gölemezli, and Karahayıt) of moderate-to-high enthalpy [38,39]. The Denizli Basin, a result of extensional tectonics characterizing the area, is approximately 70 km in length and 50 km in width, mainly located at the junction of the E-W trending Büyük Menderes Graben and the nearly NW-SE trending Gediz graben, two major tectonic remnants of the extension prevailing in the area [40–42]. Geothermal activity within the Denizli Basin mainly manifests itself along the NW-SE trending normal fault patterns, which act as major circulation pathways for the deep rising thermal fluids within the horst–graben-related fault–fracture network, heated by shallow magma bodies within the thinned crustal lithosphere of the extensional regime [43].

The Kızıldere and Tekke Hamam geothermal fields share the same lithostratigraphic sequences. The basements rocks in the area are represented by Paleozoic or older Menderes Massif Metamorphics, which is defined as a well developed metamorphic core complex composed of a crystalline core and a metasedimentary cover series [36,44–47]. The Precambrian to early Paleozoic core of the massif, which forms the basement, is mainly composed of augen gneiss, migmatites, metagranite, gabbro, and medium to high grade metamorphic schists. The cover is represented by two major Paleozoic units: (i) the Ortaköy formation, composed of mainly schist with garnet, muscovite, and biotite, and (ii) the İğdecik formation, which is mainly an alternation of marble, micaschist, and quartzite. The metamorphic complex is overlain unconformably by the Pliocene fluvial-lacustrine sedimentary formations, which are divided into four major rock series, namely from bottom to top: the Kızılburun (alternation of conglomerate, sandstone, and claystone); Sazak (limestone, marl, siltstone, and claystone alternation); Kolankaya (alternation of marl, sandstone, and siltstone); and Tosunlar (conglomerate, sandstone, and claystone) formations [40,42,48]. Quaternary alluvium, terrace deposits, and travertines cover the Pliocene sedimentary formations. Three major levels act as reservoirs in the field: (i) the low-lying gneiss levels of the Menderes massif have been identified as the deepest reservoir in the field, (ii) the intensely fractured and faulted İğdecik formation acts as a major reservoir feeding most of the wells drilled in the area, and (iii) the limestone levels of the Sazak formation act as the shallow reservoir with a rather limited lateral continuity [40,49]. The horst–graben of the area constitute the major recharge zones, with the graben bounding fault zones providing the pathways for the recharge of the thermal reservoirs [20,50].

3. Gas Sampling and Analysis

Gas samples were collected from the Tekke Hamam and Kızıldere geothermal fields during two sampling campaigns. Stable isotope analysis of carbon dioxide, methane, and nitrogen ($\delta^{13}C\text{-}CO_2$, $\delta^{13}C\text{-}CH_4$, $\delta^{2}H\text{-}CH_4$, and $\delta^{15}N\text{-}N_2$) was conducted on a total of five pool samples from Tekke Hamam (Umut-1 (a,b), Umut-2, Umut-4, and Umut-5) and four production wells from Kızıldere (KD-6, KD-13 (a,b), and KD-15), in addition to the chemical composition analysis. The gas samples from the Tekke Hamam geothermal site were collected as free gas phase utilizing an inverted funnel dipped inside the bottom of the pools to capture the bubbles released there. Gas sampling in Kızıldere, on the other hand, was performed after separation of the wellhead fluid into a gas and a water phase by means of a steam separator. Copper tubes, as well as glass tubes equipped with two stopcocks, served as sample devices. The gas was allowed to flow through the sampling devices at least for 10 min and the sample volume was replaced at least 20 times by formation gas before the sample was collected. A water trap at the sample outlet acted as a unidirectional no-return valve to minimize air contamination.

The total gas analysis was performed with a quadrupole mass spectrometer (Pfeiffer Omnistar) for N_2, O_2, CH_4, CO_2, H_2, H_2S, He, and Ar with detection limits of 1 part per million by volume for H_2, CH_4, and Ar, and 10 ppmv for O_2, N_2, and CO_2. Isobaric interferences with oxygen on the diagnostic mass over charge ratios [m/z] = 32, 33, and 34 increase the detection limit for H_2S to values of 200 ppmv [29]. Hydrocarbons were analyzed with a gas chromatograph (SRI- 8610) equipped with a flame ionization detector. Detection limits for the hydrocarbons are 1 ppmv. The stable isotope measurements on CH_4 and N_2 (^{13}C, ^{2}H, ^{15}N) were conducted via isotope ratio mass spectrometry. Stable isotope measurements were carried out at INGV-Palermo (Istituto Nazionale di Geofisica e Vulcanologia—Sezione di Palermo) laboratories. Stable carbon and hydrogen isotope compositions of CH_4 and CO_2 were measured using a Delta Plus XP IRMS equipped with a Thermo TRACE GC interfaced with Thermo GC/C III and Thermo GC/TC. $^{13}C/^{12}C$ ratios are reported as $\delta^{13}C$ values ($1\sigma = 0.1‰$) against VPDB standard and $^{2}H/^{1}H$ ratios are reported as $\delta^{2}H$ values ($1\sigma = 1‰$) against VSMOW standard. Nitrogen isotope composition ($\delta^{15}N$) was determined by using a Delta Plus XP stable isotope ratio mass spectrometer coupled with a Thermo TRACE Gas Chromatograph and a Thermo GC/C III interface, following the method proposed in [51]. $\delta^{15}N$ values ($1\sigma = 0.2‰$) are reported against Air.

4. Results and Discussions

4.1. Relative Concentrations and Chemical Composition of the Gas Samples

The chemical composition of samples taken from the Kızıldere and Tekke Hamam geothermal fields during November 2007 and September 2008 are given in Table 1. The main component of the gas samples taken from the Kızıldere and Tekke Hamam geothermal fields is represented by CO_2, changing between 96.1 and 98.4 vol.% for Kızıldere and 84.4 and 96.9 vol.% for Tekke Hamam geothermal field. Other gas components, from the highest to the least are: N_2, H_2S, CH_4, O_2, Ar, H_2, and He. CH_4 is a minor component varying around 1620 and 4300 ppmv for Kızıldere and 2844 and 4496 ppmv for Tekke Hamam. The nitrogen content varies between 1.09 and 2.91 vol.% for Kızıldere and between 1.63 and 12 vol.% for Tekke Hamam, while oxygen varies between 0.19 and 0.72 vol.% for Kızıldere and between 0.16 and 3.14 vol.% for Teke Hamam, suggesting that air contamination is negligible in most of the samples. All argon contents are much lower than the air value of 0.934%, while He abundances are ranging from 3.8 to 4.8 ppmv for Kızıldere and from 4.5 to 5.6 ppmv for Tekke Hamam, similar to that of air (5.24 ppmv, [52]). All of the gas samples, except for Umut-4a, have low amounts of O_2 (<1vol.%), which points to only little atmospheric contamination during sampling for most of the samples. Umut-4a sample, on the other hand, with its high O_2 content, accompanied by N_2/O_2 ratio similar to that of air (N_2/O_{2air}: 3.727) depicts the presence of air contamination. Based on the gas chromatographic analysis of the light hydrocarbons, the $CH_4/(C_2H_6 + C_3H_8)$ ratios vary between 101 and 860 for Kızıldere and between 36 and 43 for Tekke Hamam. The N_2/Ar ratios vary between 106 and 255 for Kızıldere and between 82 and 107 for Tekke Hamam, both fields exhibiting N_2/Ar ratios exceeding the value characteristic for atmospheric contributions (N_2/Ar~84; [53]).

Table 1. Chemical compositions of gas samples from Kızıldere and Tekke Hamam geothermal fields.

	Sample	Sampling Date	Ar (ppmv)	CH_4 (ppmv)	CO_2 (vol.%)	H_2 (ppmv)	He (ppmv)	N_2 (vol.%)	O_2 (vol.%)	Kr (ppmv)	H_2S (ppmv)	CH_4 (ppmv)	C_2H_6 (ppmv)	C_3H_8 (ppmv)	$CH_4/[C_2H_6+C_3H_8]$	N_2/Ar
Kızıldere	KD-6a	November 2007	69	2750	98.4	30	3.8	1.09	0.19	0.9	12	1620	11	5	101	158
	KD-13b	September 2008	274	2540	96.1	176	4.1	2.91	0.72	1.1	26	2962	7	3	296	106
	KD-15a	November 2007	49	4090	98.1	26	4.8	1.25	0.18	1.1	39	4301	4	1	860	253
Tekke Hamam	Umut-1a	November 2007	153	3390	96.9	103	5.3	1.63	0.16	1.1	9140	4496	80	45	36	107
	Umut-2a	November 2007	207	3700	97.2	27	5.3	1.92	0.16	1.0	3430	3731	65	40	36	92
	Umut-4a	November 2007	1330	2680	84.4	20	4.5	12	3.14	0.9	n.d.	2844	37	33	41	90
	Umut-5b	September 2008	288	4100	96.2	38	5.6	2.37	0.16	1.1	8770	3910	55	36	43	82

n.d.= not detected.

4.2. Isotopic Composition of the Gas Samples

The isotopic composition of CO_2 ($\delta^{13}C$-CO_2), CH_4 ($\delta^{13}C$-δ^2H-CH_4) (expressed as per mil (‰) vs. PDB, Pee Dee Belemnite) and N_2 ($\delta^{15}N$-N_2) (expressed as per mil (‰) vs. air), along with the gas ratios to the other components of the gas mixture ($CO_2/^3He$, $CH_4/^3He$, and $N_2/^{36}Ar$) are presented in Table 2. A total of 6 samples were analyzed for $\delta^{13}C$ on carbon dioxide and methane, along with a total of 9 samples analyzed for $\delta^{15}N$-N_2. The δ^2H analysis of CH_4, on the other hand, was conducted for two samples (KD-13a and Umut-4a).

The ^{13}C isotope values of CO_2 fall between 0.30 and 0.99 (‰ VPDB) for the samples from the Kızıldere geothermal field and between −0.95 and 1.30 (‰ VPDB) for Tekke Hamam. The $\delta^{13}C$ isotope ratio of CH_4 varies between −23.6 and −20.8‰ for Kızıldere and between −34.4 and −31.7‰ for Tekke Hamam. The δD values of CH_4 for sample KD-13a from Kızıldere is −126.7‰ and for Tekke Hamam sample Umut-4a is −143.3‰. The $\delta^{15}N$ isotope values vary broadly between −4.44 and 4.54‰ for Kızıldere and narrowly for Tekke Hamam between −0.702 and 2.75‰. The measured $CO_2/^3He$ ratios from both fields are greater than the average mantle value of 2E+09 [29]. The $CH_4/^3He$ ratios are above values characteristic for abiogenic gases ($CH_4/^3He$ ~10^6; [54]). The $N_2/^{36}Ar$ ratios are mostly greater than that of air (2.47×10^4, [55]).

Table 2. Isotopic composition of CO_2, CH_4 and N_2 of gas samples from Kızıldere and Tekke Hamam, along with their $CH_4/^3He$, $CO_2/^3He$, and $N_2/^{36}Ar$ ratios.

	Sample	Sampling Date	$\delta^{15}N$ (‰ vs. Air)	$\delta^{13}C$-CO_2 (‰ vs. PDB)	$\delta^{13}C$-CH_4 (‰ vs. PDB)	δD-CH_4 (‰ vs. PDB)	$CH_4/^3He$	* $CO_2/^3He$	$N_2/^{36}Ar$
Kızıldere	KD-6a	November 2007	4.23	0.34	−20.8		5.31×10^8	1.90×10^{11}	4.97×10^4
	KD-13a	November 2007	4.54	0.30	−23.2	−126.7	7.42×10^8	2.86×10^{11}	6.27×10^4
	KD-13b	September 2008	−2.61				7.42×10^8 *	2.86×10^{11} +	2.91×10^4
	KD-15a	November 2007	−4.44	0.99	−23.6		1.23×10^9	2.95×10^{11}	4.32×10^4
Tekke Hamam	Umut-1a	November 2007	2.75				3.52×10^8	1.01×10^{11}	3.20×10^4
	Umut-1b	September 2008	1.80	−0.95	−34.4		3.52×10^8 *	1.01×10^{11} +	2.65×10^4
	Umut-2a	November 2007	1.16	-	-			1.11×10^{11}	2.36×10^4
	Umut-4a	November 2007	0.960	−0.74	−31.7	−143.3	2.58×10^8	8.14×10^{10}	2.28×10^4
	Umut-5b	September 2008	−0.702	1.3	−32.0		3.48×10^8	8.56×10^{10}	2.46×10^4

* Data taken from [29]. + Calculated by using KD-13a, respectively, Umut-1a chemical composition data, assuming that the chemical and noble gas composition of samples from the same location does not change significantly over time.

4.3. Origin of CO_2

It is generally known that gas emanations in tectonically or volcanically active areas are typically characterized by carbon dioxide (CO_2) as the main gaseous component. The CO_2 originates in different proportions from a magmatic source, as well as from the interaction of geothermal fluids or magma with the surrounding host rock. Host rocks with potential for CO_2 release are limestone and sediments enriched in organic material. CO_2 deriving from these three sources (magmatic, limestone, and organic-rich sediments) shows distinctly different $\delta^{13}C$ isotopic composition, with $\delta^{13}C$ values (all values relative to PDB, average values in brackets) ranging from −20‰ to −40‰ (−30‰) for organic-rich sediments, −9‰ to −4‰ (−6.5‰) for MORB and −2‰ to +2‰ (±0‰) for limestone [56]. However, in order to characterize and quantify mixtures of CO_2 from these reservoirs, a further, additional parameter is required, in the composition of which the reservoir fluids also must differ. For this purpose, [56] introduced the $CO_2/^3He$ ratio as additional proxy with $CO_2/^3He = 1–2 \times 10^9$ for mantle-derived CO_2 as typically observed in MORB and ~10^{13} for CO_2 from crustal reservoirs (organic-rich sediment, limestone). It should be noted that the $CO_2/^3He$ ratio for the limestone endmember in the study area is probably in the range of 2×10^{12}, as pointed out by [29], rather than 10^{13}. However, for ease of comparison with other data sets, the subsequent estimates are based on an assumed $CO_2/^3He$ ratio endmember composition for the limestone of 10^{13}.

Several processes can alter the $CO_2/^3He$ ratio in hydrothermal fluids. Phase separation may influence the CO_2 [8,57] or the helium component, where the higher soluble CO_2 preferentially remains in the liquid phase, whereas the less-soluble helium is preferentially separated into the gas phase. [29] interpreted the low helium concentrations (0.7–2.2 ppmv) and low helium isotopic ratios ($^3He/^4He$ = 0.96–2.06 Ra) of Kızıldere geothermal fluids, both of which showing a negative correlation to temperature by tapping of a remaining liquid phase after phase separation and the consequent depletion of helium in the liquid phase. Other processes that have the potential to alter the $CO_2/^3He$ ratio in hydrothermal fluids are abiogenic reduction of CO_2 to CH_4 in the presence of reducing agents [58,59], and calcite precipitation [8,60]. Hydrothermal phase separation involving CO_2, and calcite precipitation may also impact on the $\delta^{13}C$ isotopic composition. The $CO_2/^3He$ ratios of fluid samples from Kızıldere range from 1.8 to 9.2×10^{11} and from 0.7 to 1.1×10^{11} for fluid samples from Tekke Hamam [29], higher than the average mantle value of ~2×10^9 [61]. Kızıldere samples cover a wider range of $CO_2/^3He$ ratios, while ratios from Tekke Hamam are lower and more uniform. The $\delta^{13}C$ isotope values of CO_2 fall between 0.30 and 0.99 (‰ VPDB) for the samples from the Kızıldere geothermal field (wells KD -6, KD-13 and KD-15) and between −0.95 and +1.30 (‰ VPDB) for Tekke Hamam (mofettes Umut-1, -4 and -5), respectively. In a $CO_2/^3He$ vs. $\delta^{13}C$-CO_2 diagram (Figure 2), the data of our study plot on or close to a mixing hyperbola between magmatic CO_2 and CO_2 from interaction of geothermal fluids with limestone. There is no evidence for contributions of CO_2 from organic-rich sediments. The diagram indicates that ~97% of CO_2 from samples from Tekke Hamam and ~99% of CO_2 from Kızıldere samples derives from fluid–limestone interactions, and only a small contribution is mantle-derived.

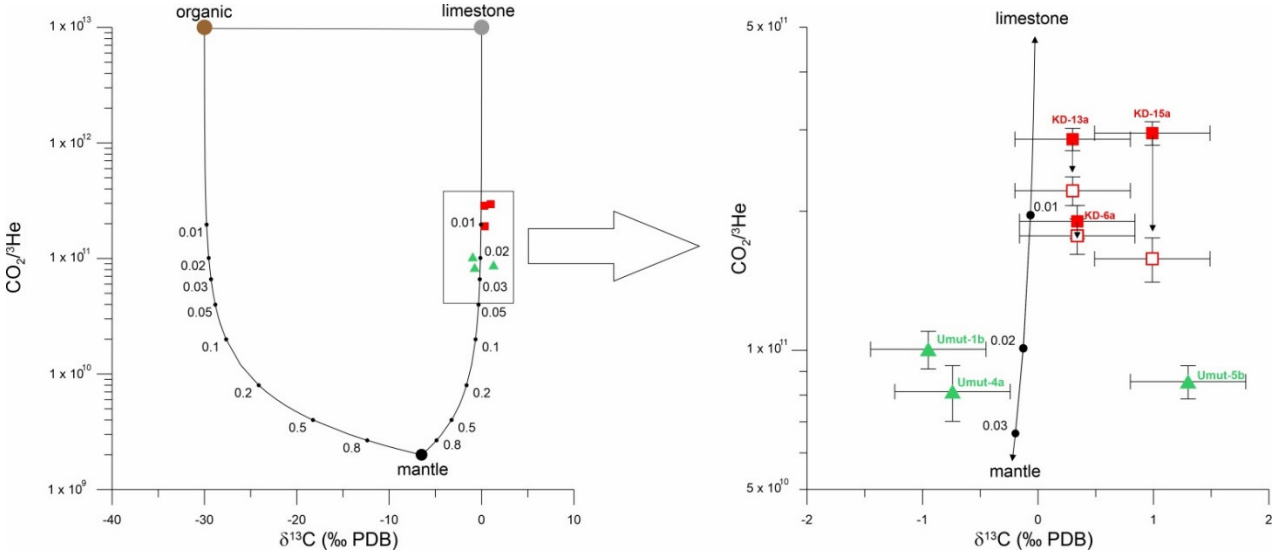

Figure 2. Diagram of $CO_2/^3He$ (data from 29) vs. $\delta^{13}C$ (CO_2, ‰ PDB) including organic, limestone and magmatic endmembers (see text for values) from [56] and mixing hyperbolas. Kızıldere samples: red squares, Tekke Hamam samples: green triangles. Right site: close up showing Kızıldere samples corrected for He phase separation effects (open squares). See text for details.

Our findings are in good agreement with [62] who proposes carbonate–magma interaction as dominant process that accounts for CO_2 in Kızıldere geothermal fluids. Ref. [27] suggested that 73–97% of CO_2 in gas and water samples from western Anatolia derives from carbonates. Similar is reported by [63] from central Anatolia with a contribution of CO_2 from fluid-limestone interaction of more than 90%.

Two different processes may account for the slightly different $CO_2/^3He$ ratios observed in Kızıldere and Tekke Hamam geothermal fluids: depletion of helium in the liquid phase after phase separation, as reported by [29] for Kızıldere samples, and the higher fluid temperatures at Kızıldere which result in amplified fluid-limestone interaction. To estimate the relevance of the first process, a correction to the $CO_2/^3He$ ratio was applied to the Kızıldere samples by calculating ^3He concentrations based on an assumed original $^3He/^4He$ ratio of 2.2 Ra (Ra = atmospheric $^3He/^4He$ ratio), as proposed by [29] rather than the observed $^3He/^4He$ ratios in Kızıldere (0.96–2.06 Ra, 29). The such-like corrected $CO_2/^3He$ ratios for Kızıldere samples are between 1.6 and 2.2 × 10^{11}(1.5–4.7 × 10^{11} for the entire dataset published by 29) which is still higher than the $CO_2/^3He$ ratios of Tekke Hamam fluid samples (0.7–1.1 × 10^{11}). Therefore, we assume that the higher temperature of geothermal fluids in Kızıldere reservoir leads to increased extraction of CO_2 from the limestone source.

4.4. Origin of Hydrocarbons

In hydrothermal fluids, methane and heavier hydrocarbons in general may derive from two possible sources: biogenic or abiogenic [64]. Biogenic methane is basically produced by microbial or thermal degradation of organic matter [65–67]. Microbial methane production such as those from wetlands and rice paddies, is peaking at temperatures lower than 50 ^{0}C, and can be related to several processes, including fermentation of acetate, dominant in freshwater sediments, and reduction of CO_2 dominant in sulfate-free zone of marine sediments [68]. The thermogenic originated methane is related to the decomposition of organic matter within sediments at temperatures peaking around 150 °C [69,70]. Abiogenic methane, on the other hand, which is methane that is not directly related to an organic precursor, generally derives from sources and processes such as (i) migration from the mantle or magmatic bodies, (ii) metamorphism of graphite bearing carbonate rocks, (iii) iron carbonate decomposition, (iv) Fischer–Tropsch-type reactions, (v) abiogenic reduction of CO_2 in volcanic-hydrothermal systems, and (vi) high temper-

ature hydrothermal serpentinization of mafic and ultramafic rocks [7,59,60,71–74]. Except for (i), all abiogenic reactions require hydrogen as reducing agent.

The stable isotopic composition of methane ($\delta^{13}C$, $\delta^{2}H$), along with the chemical composition of higher mass hydrocarbons (e.g., C_2H_6 (ethane), C_3H_8 (propane), C_4H_{10} (butane)) and their respective ratios ($C_1/[C_2+C_3]$, C_1: CH_4; C_2: C_2H_6; C_3: C_3H_8), has been used as a valuable tool for the elucidation of the possible sources of methane [67]. Typical $\delta^{13}C$ values for microbial methane vary in a wide range between −110 and −60‰ [67,75] whereas the $C_1/[C_2+C_3]$ ratio exhibit values greater than 1000 [76]. Thermogenically produced methane is characterized by more enriched $\delta^{13}C$ isotopic values, typically changing between −50 and −20‰, with $C_1/[C_2+C_3]$ ratio lower than 100 [65,67,77]. In contrast to biogenic methane, abiogenic methane, emanating from sediment free mid ocean ridge systems were suggested to have enriched $\delta^{13}C$ values (>−24‰ V-PDB), and hydrocarbon concentration ratios higher than 1000 [78–81] due to exchange with mantle carbon at high temperatures.

The CH_4 content of the Kızıldere and Tekke Hamam gases generally vary between 1600 and 4500 ppmv which is very low compared to the dominant CO_2 characteristic of the gases (reaching up to 98 vol.%), but surprisingly high compared to typical high-enthalpy geothermal gases of magmatic origin. The relatively high content of CH_4 and $C_1/[C_2+C_3]$ values observed in most of the gas samples from both fields were previously attributed to an input of possibly thermogenic methane [29], given the fact that methane from pure magmatic gases is very low, almost free of methane [82]. The $\delta^{13}C$ isotopic composition, together with the gas compositional ratio of hydrocarbons $C_1/[C_2+C_3]$, also underpins the organic nature for the source of methane (Tables 1 and 2). Figure 3. shows the distribution of the gas samples on a modified so-called "Bernard diagram".

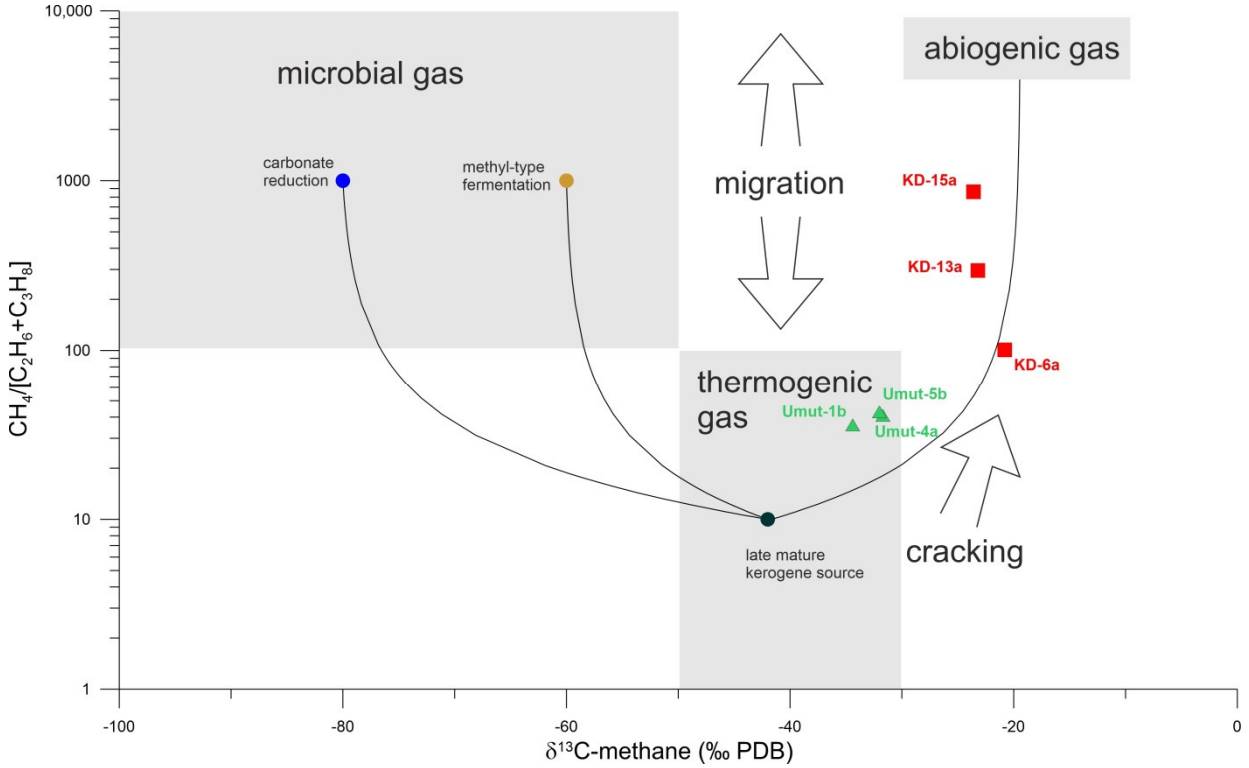

Figure 3. $CH_4/[C_2H_6+C_3H_8]$ vs. $\delta^{13}C$ diagram ("Bernhard-diagram") including mixing lines of hydrocarbons from late mature kerogene source (black circle) with microbial gas from carbonate reduction (blue circle) and methyl-type fermentation (brown circle, values from [67]), as well as mixing with abiogenic hydrocarbons. Tekke Hamam samples plot in the thermogenic field, but show indication for mixing with abiogenic gas or with gas from secondary cracking. In comparison, samples from Kızıldere are more depleted in ethane and propane and $\delta^{13}C$-methane is isotop-

ically heavier, demonstrating a higher contribution of the abiogenic/secondary cracking component.

As can be seen from the diagram, both Kızıldere and Tekke Hamam samples localize along the thermogenic methane field ($\delta^{13}C$ isotopic values changing between −34 and −20‰), possibly suggesting high temperature gas release from organic rich sediments. The possibility of a microbial methane source was previously eliminated based on the high amounts of higher mass hydrocarbons (C_{2+}), as these species are not characteristic of microbial activity, and therefore cannot be observed in high temperature systems. The diagram also presents a different distribution for the geothermal fields. The samples from Tekke Hamam have hydrocarbon ratios varying tightly around 40 ($C_1/C_2+C_3 < 100$), and $\delta^{13}C$ values more to the negative side, which is in conformity with methane produced via thermal degradation of organic matter. The gas samples from Kızıldere, on the other hand, display a scattered distribution of hydrocarbon gas ratio (mostly above 100), with $\delta^{13}C$ values lying along the transition zone from thermogenic to abiogenic origin. The wide scatter in the hydrocarbon ratio probably suggests the existence of additional temperature dependent secondary processes such as (i) cracking of long chain hydrocarbons and/or (ii) enhanced production of methane from overmature kerogen at high temperatures, as was suggested in previous studies [29,83], both of which would also affect the $\delta^{13}C$ isotopic values of methane towards more heavy values. [84] report methane concentrations (0.013–2.53 vol.-% with average value of 0.82 vol.-%) and $\delta^{13}C$ isotopic composition of methane (−40 to −26.8‰ PBD) from the Acoculco caldera geothermal system in Mexico, similar to the values of the present study, and attributes these findings with a deep thermogenic origin of methane. [63] found up to 0.1 vol.-% methane with $\delta^{13}C$ values of −24‰ (PBD) in geothermal gas emanations in Central Anatolia, which the authors also interpreted with a thermogenic origin.

The heavier $\delta^{13}C$ isotopic values, together with hydrocarbon ratios greater than 100, however, can also be explained by an abiogenic component (e.g., 58,59) that can be evaluated based on the correlation between $\delta^{13}C$-CH_4 isotopic ratios and the elemental ratio of CH_4 to ^3He, which is a major tracer for fluids from the mantle [85]. Figure 4 shows the relationship between $\delta^{13}C$-CH_4 and $CH_4/^3He$ ratios, which was used in studies before [54,86]. Thermogenic and abiogenic methane have been assigned values of $CH_4/^3He$ in the range of 10^{13} and 5×10^6, respectively [54]. The samples from our study reveal $CH_4/^3He$ ratios between 5×10^8 and 1.3×10^9 for Kızıldere fluids and somewhat lower values ($2–3 \times 10^8$) for those of Tekke Hamam, respectively. Both Kızıldere and Tekke Hamam gases display mixture between two possible end members: thermogenic methane from organic sources of different maturity, and abiogenic methane. The comparison of $\delta^{13}C$ and H/D values of methane (Figure 5) show similar behavior. Given that the CO_2 content in Western Anatolian thermal fluids have been shown to be a mixture of dominant crustal (limestone) and minor mantle contribution, based on the $\delta^{13}C$-CO_2 and $CO_2/^3He$ ratios of gases (see Figure 2), it is possible that the CH_4 content can also be represented by a mixture of a dominant crustal (thermogenic) and minor mantle (abiogenic) source.

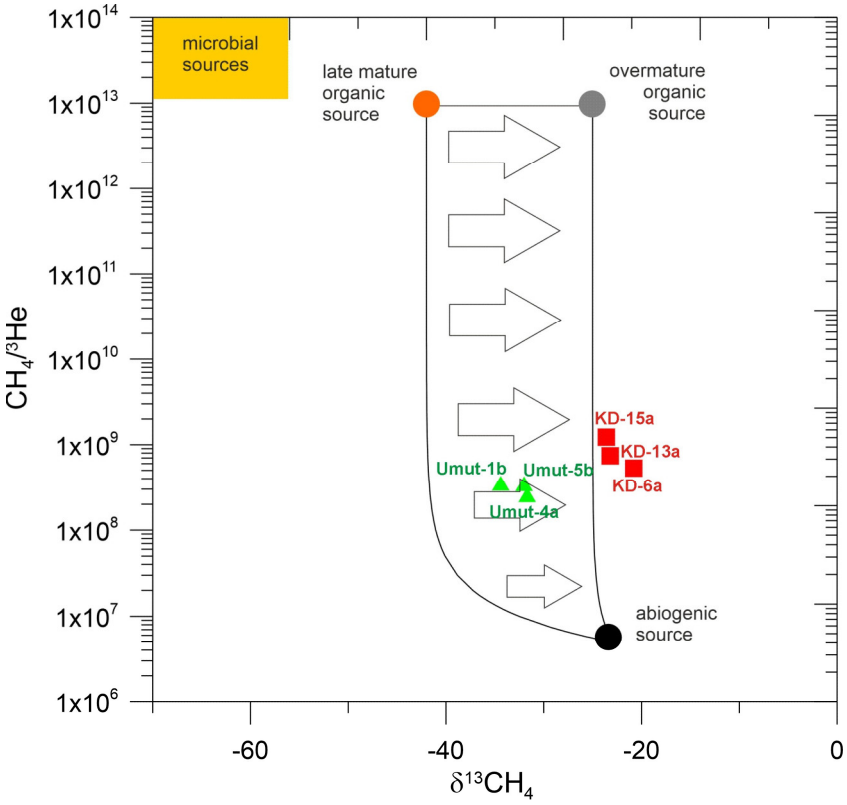

Figure 4. Correlation diagram between $\delta^{13}C$ of methane and $CH_4/^3He$ ratios, modified from [54]. $\delta^{13}C$ values of methane from kerogen endmembers with different maturities from [68], $\delta^{13}C$ values of abiogenic methane and $CH_4/^3He$ ratios from [54]. Kızıldere samples: red squares. Tekke Hamam samples: green triangles. Both Tekke Hamam and Kızıldere sample show mixing between abiogenic and thermogenic methane. Tekke Hamam samples contain methane from a less mature organic source. Arrows indicate increasing thermal maturity of the source of thermogenic methane.

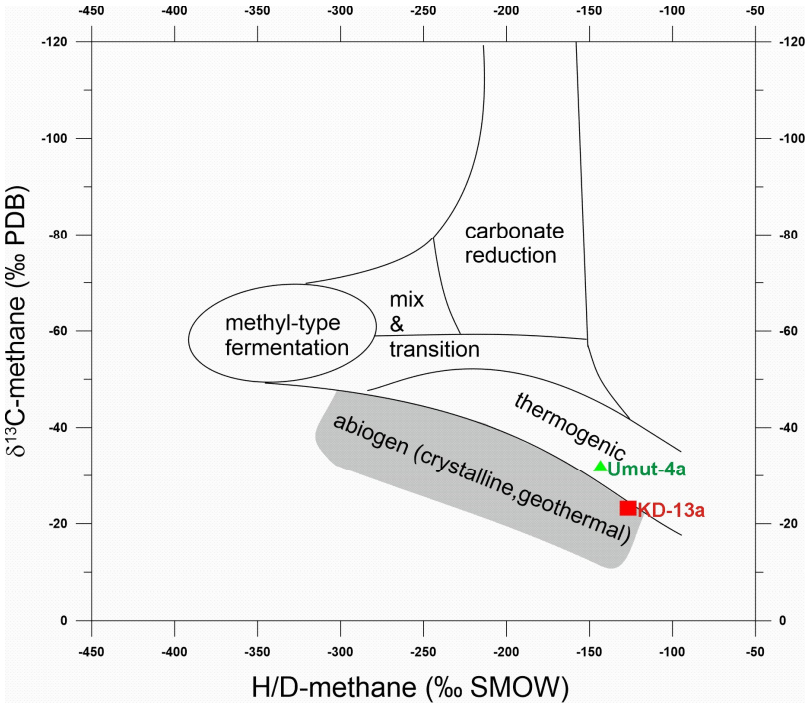

Figure 5. Diagram between $\delta^{13}C$ and H/D values of methane ("Schoell-diagram", 66). Kızıldere sample (red square) plots on the mixing line between thermogenic and abiogenic methane. Tekke Hamam sample (green triangle) in the thermogenic field.

Based on the geodynamic setting of our study area, the organic source material of thermogenic methane is most likely hosted in the thick Pliocene sedimentary cover. The minor abiogenic origin for methane, on the other hand, can be related to either (i) mantle source (contributing up to ~4% of total-CO_2 [27] and 35% of total-He [29] gas inventories in Western Anatolian fluids), or ii) inorganic reactions, such as Fischer–Tropsch.

4.5. Origin of N_2

Nitrogen constitutes the major component of air and is found as a trace component within rocks. N_2, like O_2 and Ar, can be considered to be derived from the atmosphere upon dissolution in groundwater during meteoric recharge of geothermal systems. Other than atmospherically derived nitrogen, non–atmospheric components of nitrogen within thermal fluids can be present due to contributions from different sources, such as sedimentary rocks containing organic matter, inorganic nitrogen in sediments, metamorphism of sedimentary rocks and mantle derived nitrogen [87–89].

The gas samples taken from Kızıldere and Tekke Hamam geothermal fields have N_2 values varying between 1.09 and 2.91 vol.%, and between 1.63 and 12 vol.%, respectively, with N_2 being the second dominant component after CO_2. The ratio of N_2 to Ar and O_2 can be used as an initial parameter for the delineation of a possible existence of a – nitrogen component within a thermal fluid. Especially, the ratio of N_2 to Ar has been used as an indicator for the origin of nitrogen in natural gases [90], volcanic gases [91,92] and sedimentary rocks [93]. The N_2/Ar ratio of the gases from Kızıldere and Tekke Hamam vary between 106 and 253, and between 82 and 107, respectively. Given that the N_2/Ar ratio of air saturated water and air is 38 (at 20 °C) and 83.6 [53], respectively, it is apparent that nearly all of the gas samples exhibit a contribution from a non–atmospheric nitrogen component, in addition to N_2 derived from atmosphere upon dissolution through the recharge of the thermal reservoir or air by contamination during sampling. Only for the samples Umut-4a and Umut-5b, exhibiting N_2/Ar values similar to that of air, can a sole atmospheric nitrogen origin be suggested; therefore, eliminating any source of non–atmospheric contribution within these samples. Particularly, the N_2/O_2 ratio of sample Umut-4a (close to the value of air: 3.7) shows that there is also a considerable amount of air contamination, possibly due to improper sampling of this gas. Both samples also exhibit $\delta^{15}N$ (‰ vs. air) values close to air, with $\delta^{15}N$ = +0.96‰ for Umut-4a and −0.702‰ for Umut-5b, respectively.

The stable isotopic composition of nitrogen $\delta^{15}N$ (‰ vs. Air) has been used as a tracer for the delineation of the possible non–atmospheric nitrogen components present within terrestrial fluids issuing from various tectonic settings [94,95]. Nitrogen derived from (i) sediments (inorganic) of continental crust and/or subducted oceanic slab have $\delta^{15}N$ values around +7‰, [55], (ii) mantle derived N_2, including unaltered ocean crust and N_2 degassed from the upper mantle exhibit $\delta^{15}N$ values close to −5‰, [89], (iii) nitrogen related to organic sources of different degrees of maturity have values in the negative range, reaching −19‰ [96]. Since the isotopic characteristics of different nitrogen reservoirs within the subsurface coincide at some level, it is the general trend to compare the $\delta^{15}N$ isotopic values with those of the elemental ratios, such as $N_2/^{36}Ar$ [54,55] and $N_2/^{3}He$ [95] for the delineation of the possible nitrogen sources.

Figure 6 shows the diagram of $\delta^{15}N$ vs. $N_2/^{36}Ar$ ratio, with the possible end members (Air, Air Saturated Water, Mantle, Sediment; the endmember values for both $\delta^{15}N$ and $N_2/^{36}Ar$ are taken from [55]). Both Kızıldere and Tekke Hamam gases are located inside a mixing zone of the end member components (air, mantle, sediment), therefore calling for the existence of both sedimentary and mantle contributions for the gases, in addition to a constant atmospheric component that entered the geothermal system via reservoir recharge. The wide distribution of the Kızıldere gas samples ($\delta^{15}N$: −4.44 and 4.54‰ vs. air), showing values similar to that of both sedimentary and mantle nitrogen sources, however, possibly necessitates further arguments regarding possible physicochemical processes affecting the gases on their journey from the deep source to the surface. Especially,

the effects of isotopic fractionation in relation to gas ascent in Kızıldere can be acting on these gases to a varying degree. In this context, it seems remarkable that samples from the Kızıldere well 13 show significant variations from +4.51‰ in November 2007 (sample Kızıldere-13a) to −2.61‰ in September 2008.

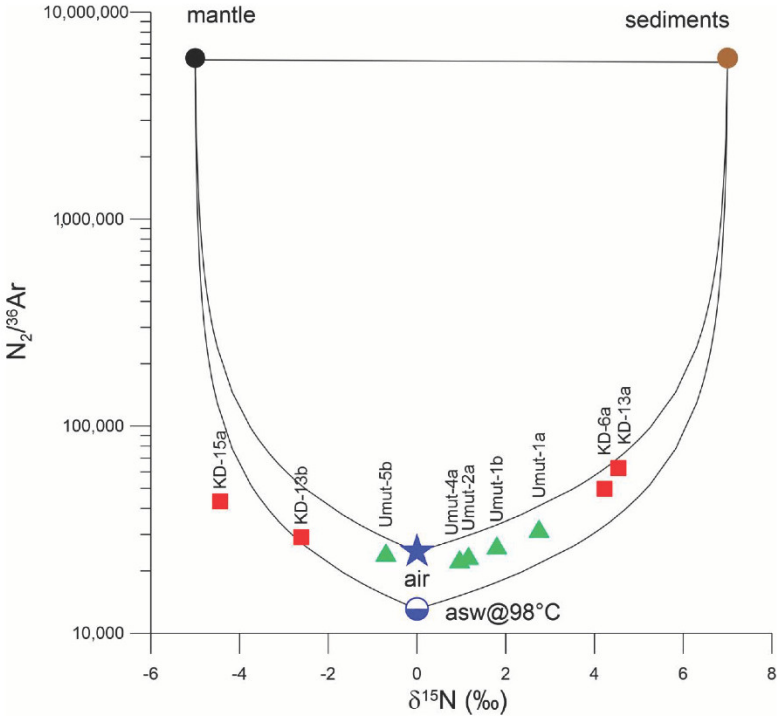

Figure 6. $N_2/^{36}Ar$ ratios vs. $\delta^{15}N$ diagram, with possible endmembers air, air-saturated water (asw@98 °C = air-saturated water at 98 °C. The $N_2/^{36}Ar$ ratio in air-saturated water is lower than in air, which is due to the higher solubility of argon in water compared to nitrogen), mantle, and organic-rich sediments (modified from [54]). Most Kızıldere and all Tekke Hamam gas samples fall inside a mixing zone of both atmospheric endmembers and one deep endmember. Kızıldere samples: red squares, Tekke Hamam samples: green triangles.

4.6. Reservoir Temperature Evaluation

The temperature of deep geothermal reservoir conditions can be highlighted based on temperature dependent isotopic fractionation between different compounds in geothermal fluids [97]. Various geothermometers have been designed based on the concept of isotopic fractionation, among which the CO_2-CH_4 isotope geothermometer has been used widely and reliably until now [5,9,97]. This geothermometer, based on the calculated carbon isotope fractionation factors between CO_2 and CH_4 via spectroscopic data [98] assumes that (i) carbon isotope fractionation reaches equilibrium between CO_2 and CH_4, and (ii) there exists a symbiotic relationship between CO_2 and CH_4. The results of this geothermometer generally yield temperatures 50–150 °C higher than those encountered in drillholes [99].

$$^{12}CO_2 + {}^{13}CH_4 = {}^{13}CO_2 + {}^{12}CH_4$$

The temperature estimations, according to the temperature dependent relation of the CO_2-CH_4 isotope geothermometer given below indicates temperatures 20–40 °C higher at Tekke Hamam (compared to wells with temperatures reaching 170 °C, [18]) and 100–160 °C at Kızıldere than measured bottomhole temperatures (Table 3).

$$T = 22166/(13.86 + {}^{13}C(CO_2\text{-}CH_4)) - 273$$

Compared to previous temperature calculations performed by [29] via the use of hydrocarbon gas ratio geothermometry [83], the obtained results are higher for Kızıldere.

The greater temperature discrepancy between the measured temperatures and those derived from carbon isotopes at Kızıldere could be due to one or a combination of the following processes: (i) a faster ascent through wellbores at Kızıldere that hampers equilibrium achievement more than at Tekke Hamam, where fluids ascent slowly through fractures and faults, (ii) catalytic effects: Higher concentration of sulphuric species in geothermal gases from Tekke Hamam suggests a stronger interaction with metal sulphides that may act as catalysts, and (iii) secondary cracking processes of hydrocarbons that would alter the pristine $\delta^{13}C$ signature of CH_4 towards higher values. Overall, the results obtained by this geothermometer possibly reflect temperatures at deeper levels than those penetrated by the drillholes.

Table 3. Results of isotope geothermometry calculations for Kızıldere and Tekke Hamam gas samples.

					CO_2_CH_4 Isotope Geothermometer	**Hydrocarbon Composition Geothermometer [29]**
	Sample	**$\delta^{13}C$-CO_2 (‰ vs. VPDB)**	**$\delta^{13}C$-CH_4 (‰vs. VPDB)**	**Bottom–hole Temp (°C)**	**Calculated Temp (°C)**	**Calculated Temp (°C)**
Kızıldere	KD-6a	0.34	−20.8	194	347	224
	KD-13a	0.3	−23.2	198	309	250
	KD-15a	0.99	−23.6	208	294	274
Tekke Hamam	Umut-1b	−0.95	−34.4	-	195	-
	Umut-4a	−0.74	−31.7	-	219	-
	Umut-5b	1.3	−32.01	-	197	-

5. Conclusions

In this study, we presented the stable isotopic evaluation of the gases (CO_2, CH_4 and N_2) sampled from two neighboring geothermal fields located within the Büyük Menderes Graben, Turkey. Our findings are presented as follows:

i) The carbon isotopic ($\delta^{13}C$) composition of CO_2, together with its ratio to ^3He, points to a dominant limestone source and an accompanying minor magmatic component for gas samples collected from both fields.

ii) The carbon isotopic ($\delta^{13}C$) composition of CH_4, representing a minor gas component in the gas samples, reveals a dominant thermogenic character, with additional secondary processes (e.g., cracking of long chain hydrocarbons or input of abiogenic methane from deep sources), particularly effective on gas samples collected from the Kızıldere geothermal field.

iii) The nitrogen isotopic ($\delta^{15}N$) composition, along with its elemental ratio to Ar, has pointed out to the existence of a non–atmospheric nitrogen component within both fields, possibly representing a mixture of crustal and mantle sources.

iv) The thick sedimentary cover, overlying the deep metamorphic basement, is the likely source for both the dominant CO_2 and the minor CH_4 and N_2 components issuing from both fields. A wider array of sampling points for both gas and isotopic compositions will better address the likely sources of the gases issuing from both fields.

v) The isotope geothermometry calculations have revealed a big temperature difference for Kızıldere and a rather small difference for Tekke Hamam. The difference that is more prominent for Kızıldere can possibly highlight the lack of equilibrium conditions due to fast gas ascent through the wellbores of Kızıldere and/or secondary cracking processes for hydrocarbons, which would alter the pristine $\delta^{13}C$ signature of CH_4 towards higher values.

Author Contributions: Conceptualization, S.S., T.W., and N.G. and methodology, F.G. All authors have read and agreed to the published version of the manuscript.

Funding: This research received no external funding.

Data Availability Statement: Not applicable.

Acknowledgments: This work is part of a Turkish–German cooperation project funded by The Scientific and Technological Research Council of Turkey (TUBİTAK, Project No. 106Y200) and the Deutsche Forschungsgemeinschaft (DFG-Nr: 446 TÜR 113/1). We would like to express our sincere thanks to Umut Thermal Resort and Zorlu Energy Group for making it possible for us to access the sampling sites and for their help during sampling.

Conflicts of Interest: The authors declare no conflicts of interest.

References

1. Panichi, C.; Gonfiantini, R. Environmental isotopes in geothermal studies. *Geothermics* **1977**, *6*, 143–161.
2. Sano, Y.; Urabe, A.; Wakita, H.; Chiba, H.; Sakai, H. Chemical and isotopic compositions of gases in geothermal fluids in Iceland. *Geochem. J.* **1985**, *19*, 135–148.
3. Minissale, A.; Evans, W.C.; Magro, G.; Vaselli, O. Multiple source components in gas manifestations from north-central Italy. *Chem. Geol.* **1997**, *142*, 175–192.
4. Horita, J. Carbon isotope exchange in the system CO_2-CH_4 at elevated temperatures. *Geochim. Cosmochim. Acta.* **2001**, *65*, 1907–1919.
5. Gherardi, F.; Panichi, C.; Gonfiantini, R.; Magro, G.; Scandiffio, G. Isotope systematics of C-bearing gas compounds in the geothermal fluids of Larderello, Italy. *Geothermics* **2005**, *34*, 442–470.
6. Chen, G.; Wang, G.; Sun, Z.; Liu, J. The isotopic and chemical characteristics of geothermal fluids from two selected hot spring areas in Jiangxi Province, SE-China. In Proceedings of the World Geothermal Congress, Bali, Indonesia, 25–30 April 2010.
7. Tassi, F.; Fiebig, J.; Vaselli, O.; Nocentini, M. Origins of methane discharging from volcanic-hydrothermal, geothermal and cold emissions in Italy. *Chem. Geol.* **2012**, *310–311*, 36–48.
8. Roulleau, E.; Tardani, D.; Sano, Y.; Takahata, N.; Vinet, N.; Bravo, F.; Muñoz, C.; Sanchez, J. New insight from noble gas and stable isotopes of geothermal/hydrothermal fluids at Caviahue-Copahue Volcanic Complex: Boiling steam separation and water-rock interaction at shallow depth. *J. Volcanol. Geotherm. Res.* **2016**, *328*, 70–83.
9. Pang, J.; Pang, Z.; Lv, M.; Tian, J.; Kong, Y. Geochemical and isotopic characteristics of fluids in the Niutuozhen geothermal field, North China. *Environ. Earth Sci.* **2018**, *77*, 12.
10. Alam, B.Y.C.S.S.S.; Itoi, R.; Taguchi, S.; Saibi, H.; Yamashiro, R. Hydrogeochemical and isotope characterization of geothermal waters from the Cidanau geothermal field, West Java, Indonesia. *Geothermics* **2019**, *78*, 62–69.
11. Daskalopoulou, K.; Gagliano, A.L.; Calabrese, S.; Li Vigni, L.; Longo, M.; Kyriakopoulos, K.; Pecoraino, G.; D'Alessandro, W. Degassing at the Volcanic/Geothermal System of Kos (Greece): Geochemical Characterization of the Released Gases and CO_2 Output Estimation. *Geofluids* **2019**, *2019*, 16.
12. Rahayudin, Y.; Kashiwaya, K.; Tada, Y.; Iskandar, I.; Koike, K.; Atmaja, R.; Herdianita, N. On the origin and evolution of geothermal fluids in the Patuha Geothermal Field, Indonesia based on geochemical and stable isotope data. *Appl. Geochem.* **2020**, *114*, 104530.
13. Tiwari, S.K.; Gupta, A.K.; Asthana, A.K.L. Evaluating CO_2 flux and recharge source in geothermal springs, Garhwal Himalaya, India: Stable isotope systematics and geochemical proxies. *Environ. Sci. Pollut. Res.* **2020**, *27*, 14818–14835.
14. Eymold, W.; Walsh, T.; Moortgat, J.; Grove, B.; Darrah, T. Constraining fault architecture and fluid flow using crustal noble gases. *Appl. Geochem.* **2021**, *129*, 104954.
15. Kindap, A.; Kaya, T.; Haklıdır, F.S.T.; Bükülmez, A.A. Privatization of Kızıldere geothermal power plant and new approaches for field and plant. In Proceedings of World Geothermal Congress, Bali, Indonesia, 25–30 April 2010; pp. 1–4.
16. Akkuş, İ.; Akıllı, H.; Ceyhan, S.; Dilemre, A.; Tekin, Z. *Turkey Geothermal Resources Inventory*; Directorate of Mineral Research and Exploration Institute of Turkey (MTA): Ankara, Turkey, 2005.
17. Haklıdır, F.S.T.; Şengün, R.; Haizlip, J.R. The Geochemistry of the deep reservoir wells in Kızıldere (Denizli City) geothermal field (Turkey). In Proceedings of the World Geothermal Congress, Melbourne, Australia, 19–24 April 2015.
18. Süer, S. Geochemical Monitoring of the Seismic Activity and Noble Gas Characterization of the Geothermal Fields along the Eastern Segment of the Büyük Menderes Graben. Ph.D. Thesis, Middle East Technical University, Ankara, Turkey, 2010.
19. Dominco, E.; Samilgil, E. The geochemistry of the Kizildere geothermal field, in the framework of the Saraykoy–Denizli geothermal area. *Geothermics* **1970**, *2*, 553–560.
20. Şimsek, Ş. Geothermal model of Denizli, Sarayköy-Buldan Area. *Geothermics* **1985**, *14*, 393–417.
21. Gökgöz, A. Geochemistry of the Kızıldere-Tekke Hamam-Buldan-Pamukkale geothermal fields, Turkey. In *Geothermal Training Programme Orkustofnun*; United Nations University: Reykjavik, Iceland, 1998.

22. Özgur, N. Hydrogeochemical and isotope geochemical features of the thermal waters of Kızıldere, Salavatlı and Germencik in the rift zone of the Büyük Menderes, Western Anatolia, Turkey: Preliminary studies. In Proceedings of the 9th International Symposium on Water-Rock Interaction, Taupo, New Zealand, 30 March–3 April 1998; pp. 645–648.
23. Mutlu, H.; Güleç, N. Hydrogeochemical outline of thermal waters and geothermometry applications in Anatolia, Turkey. *J. Volcanol. Geotherm. Res.* **1998**, *85*, 495–515.
24. Güleç, N.; Hilton, D.R.; Mutlu, H. Helium isotope variations in Turkey: Relations to tectonics, volcanism and recent seismic activities. *Chem. Geol.* **2002**, *187*, 129–142.
25. Şimşek, Ş. Hydrogeological and isotopic survey of geothermal fields in the Büyük Menderes graben, Turkey. *Geothermics* **2003**, *32*, 669–678.
26. Moeller, P.; Dulski, P.; Özgür, N. Partitioning of rare earths and some major elements in the Kızıldere geothermal field, Turkey. *Geothermics* **2008**, *37*, 132–156.
27. Mutlu, H.; Güleç, N.; Hilton, D.R. Helium–carbon relationships in geothermal fluids of western Anatolia, Turkey. *Chem. Geol.* **2008**, *247*, 305–321.
28. Haklıdır, F.S.T.; Akın, T.; Güney, A.; Bükülmez, A.A. Geochemistry of fluids in new wells of Kizildere geothermal field in Turkey. In Proceedings of the Thirty-SixthWorkshop on Geothermal Reservoir Engineering Stanford University, Stanford, CA, USA, 31 January–2 February 2011.
29. Wiersberg, T.; Süer, S.; Güleç, N.; Erzinger, J.; Parlaktuna, M. Noble gas isotopes and the chemical composition of geothermal gases from the eastern part of the Büyük Menderes Graben (Turkey). *J. Volcanol. Geotherm. Res.* **2011**, *208*, 112–121.
30. Baba, A.; Sözbilir, H. Source of arsenic based on geological and hydrogeochemical properties of geothermal systems in Western Turkey. *Chem. Geol.* **2012**, *334*, 364–377.
31. Karakuş, H.; Şimşek, Ş. Tracing deep thermal water circulation systems in the E–W trending Büyük Menderes Graben, western Turkey. *J. Volcanol. Geotherm. Res.* **2013**, *252*, 38–52.
32. Tarcan, G.; Özen, T.; Gemici, Ü.; Çolak, M.; Karamanderesi, İ.H. Geochemical assessment of mineral scaling in Kızıldere geothermal field, Turkey. *Environ. Earth Sci.* **2016**, *75*, 1317.
33. Süer, S.; Wiersberg, T.; Güleç, N.; Erzinger, J.; Parlaktuna, M. Real-time gas monitoring at the Tekke Hamam geothermal field (Western Anatolia, Turkey): An assessment in relation to local seismicity. *Nat. Hazard.* **2020**, *104*, 1655–1678.
34. Mc Kenzie, D.P. Active tectonics of the Mediterranean region. *Geophys. J. Int.* **1972**, *30*, 109–185.
35. Dewey, J.F.; Şengör, A.M.C. Aegean sea and surrounding regions: Complex multiplate and continuum tectonics in a convergent zone. *Geol. Soc. Am. Bull.* **1979**, *90*, 84–92.
36. Bozkurt, E. Neotectonics of Turkey—A synthesis. *Geodin. Acta* **2001**, *14*, 3–30.
37. Bozkurt, E.; Mittwede, S.K. Introduction: Evolution of Neogene extensional tectonics of western Turkey. *Geodin. Acta* **2005**, *18*, 153–165.
38. Alçiçek, H.; Bülbül, A.; Alçiçek, M.C. Hydrogeochemistry of the thermal waters from the Yenice Geothermal Field (Denizli Basin, Southwestern Anatolia, Turkey). *J. Volcanol. Geotherm. Res.* **2016**, *309*, 118–138.
39. Alçiçek, H.; Bülbül, A.; Brogi, A.; Liotta, D.; Ruggieri, G.; Capezzuoli, E.; Meccheri, M.; Yavuzer, İ.; Alçiçek, M.C. Origin, evolution and geothermometry of the thermal waters in the Gölemezli Geothermal Field, Denizli Basin (SW Anatolia, Turkey). *J. Volcanol. Geotherm. Res.* **2018**, *349*, 1–30.
40. Şimsek, Ş. *Denizli, Kızıldere, Tekkehamam, Tosunlar, Buldan ve Yenice Alanları jeolojisi ve Jeotermal Enerji Olanakları*; Report No. 7486; General Directorate of Mineral Research and Exploration (MTA): Ankara, Turkey, 1984 (in Turkish).
41. Koçyiğit, A. The Denizli graben-horst system and the eastern limit of western Anatolian continental extension: Basin fill, structure, deformational mode, throw amount and episodic evolutionary history, SW Turkey. *Geodin. Acta* **2005**, *18*, 167–208.
42. Alçiçek, H.; Varol, B.; Özkul, M. Sedimentary facies, depositional environments and palaeogeographic evolution of the Neogene Denizli Basin, SW Anatolia, Turkey. *Sediment. Geol.* **2007**, *202*, 596–637.
43. Güleç, N.; Hilton, D.R. Helium and heat distribution in western Anatolia, Turkey: Relationship to active extension and volcanism. *Spec. Pap.-Geol. Soc. Am.* **2006**, *409*, 305–319.
44. Şengör, A.M.C.; Yılmaz, Y. Tethyan evolution of Turkey: A plate tectonic approach. *Tectonophysics* **1981**, *75*, 181–241.
45. Şengör, A.M.C.; Satır, M.; Akkök, R. Timing of the tectonic events in the Menderes Massif, western Turkey: Implications for tectonic evolution and evidence for Pan-African basement in Turkey. *Tectonics* **1984**, *3*, 693–707.
46. Okay, A.I. High pressure/low temperature metamorphic rocks of Turkey. *Geol. Soc. Am. Bull.* **1986**, *164*, 333–347.
47. Bozkurt, E.; Park, R.G. Southern Menderes Massif: An incipient metamorphic core complex in western Anatolia, Turkey. *J. Geol. Soc. Lond.* **1994**, *151*, 213–216.
48. Sun, S. *Denizli-Uşak Arasının Jeolojisi ve Linyit Olanakları*; Report No.9985; General Directorate of Mineral Research and Exploration (MTA): Ankara, Turkey, 1990 (in Turkish).
49. Ölmez, E.; Manav, E.; Ertürk, I.; Çetiner, H.L.; Süzük, H.; Bora, A.; Yıldırım, N. *Denizli-Kızıldere TH-2 Nolu Jeotermal Reenjeksiyon Sondajı Kuyu Bitirme Raporu;* Report No. 864; General Directorate of Mineral Research and Exploration (MTA): Ankara, Turkey, 1998 (in Turkish).
50. Şimsek, Ş.; Yıldırım, N.; Gülgör, A. Development and environmental effects of the Kızıldere Geothermal Power project, Turkey. *Geothermics* **2005**, *34*, 239–256.

51. Grassa, F.; Capasso, G.; Oliveri, Y.; Sollami, A.; Carreira, P.; Carvalho, M.R.; Marques, J.M.; Nunes, J.C. Nitrogen isotopes determination in natural gas: Analytical method and first results on magmatic, hydrothermal and soil gas samples. *Isot. Environ. Health Stud.* **2010**, *46*, 141–155.
52. Ozima, M.; Podosek, F.A. *Noble Gas Geochemistry*; Cambridge University Press: Cambridge, UK, 2002; p. 367.
53. Giggenbach, W.F. The use of gas chemistry in delineating the origin of fluids discharges over the Taupo Volcanic Zone: A review. In Proceedings of the International Volcanological Congress, Proceedings Symposium 5, Hamilton, New Zealand, 1–9 February 1986; pp. 47–50.
54. Sano, Y.; Kinoshita, N.; Kagoshima, T.; Takahata, N.; Sakata, S.; Toki, T.; Kawagucci, S.; Waseda, A.; Lan, T.; Wen, H.; et al. Origin of methane-rich natural gas at the West Pacific convergent plate boundary. *Sci. Rep.* **2017**, *7*, 15646.
55. Sano, Y.; Takahata, N.; Nishio, Y.; Fischer, T.P.; Williams, S.N. Volcanic flux of nitrogen from the Earth. *Chem. Geol.* **2001**, *171*, 263–271.
56. Sano, Y.; Marty, B. Origin of carbon in fumarolic gas from island arcs. *Chem. Geol.* **1995**, *119*, 264–274.
57. Ray, M.C.; Hilton, D.R.; Muñoz, J.; Fischer, T.P.; Shaw, A.M. The effects of volatile recycling, degassing and crustal contamination on the helium and carbon geochemistry of hydrothermal fluids from the Southern Volcanic Zone of Chile. *Chem. Geol.* **2009**, *266*, 38–49.
58. Fiebig, J.; Woodland, A.B.; Spangenberg, J.; Oschmann, W. Natural evidence for rapid abiogenic hydrothermal generation of CH_4. *Geochim. Cosmochim. Acta* **2007**, *71*, 3028–3039.
59. Fiebig, J.; Woodland, A.B.; D'Alessandro, W.; Püttmann, W. Excess methane in continental hydrothermal emissions is abiogenic. *Geology* **2009**, *37*, 495–498.
60. Hilton, D.R.; Gronvold, K.; Sveinbjornsdottir, A.E.; Hammerschmidt, K. Helium isotope evidence for off-axis degassing of the Icelandic hotspot. *Chem. Geol.* **1998**, *149*, 173–187.
61. Marty, B.; Jambon, A. C/^{3}He in volatile fluxes from the solid Earth: Implications for carbon geodynamics. *Earth Planet. Sci. Lett.* **1987**, *83*, 16–26.
62. Özgür, N. Geochemical signature of the Kızıldere geothermal field, Western Anatolia, Turkey. *Int. Geol. Rev.* **2002**, *44*, 153–163.
63. Hosgörmez, H.; Özgan, D. Origin of carbon dioxide occurrences in Central Anatolia (Turkey). *Geochem. J.* **2015**, *49*, 1–9.
64. Welhan, J.A. Origins of methane in hydrothermal systems. *Chem. Geol.* **1988**, *71*, 183–198.
65. Bernard, B.B. Light Hydrocarbons in Marine Sediments. Ph.D. Thesis, A&M University, College Station, TX, USA, 1978.
66. Schoell, M. Genetic characterisation of natural gases. *AAPG Bull.* **1983**, *67*, 2225–2238.
67. Whiticar, M.J. Correlation of natural gases with their sources, Chapter 16: Part IV. In *Memoir-M60: The Petroleum System: From Source to Trap*; Magoon, L.B., Dow, W.G., Eds.; American Association of Petroleum Geologists: Tulsa, OK, USA, 1994, pp 261–283.
68. Whiticar, M.J. Carbon and hydrogen isotope systematics of bacterial formation and oxidation of methane. *Chem. Geol.* **1999**, *161*, 291–314.
69. Hunt, J.M. *Petroleum Geochemistry and Geology*; W.H. Freeman and Co.: New York, NY, USA, 1996; p. 743.
70. Etiope, G.; Fridriksson, T.; Italiano, F.; Winiwarter, W.; Theloke, J. Natural emissions of methane from geothermal and volcanic sources in Europe. *J. Volcanol. Geotherm. Res.* **2007**, *165*, 76–86.
71. Sherwood Lollar, B.; Westgate, T.; Ward, J.A.; Slater, G.F.; Lacrampe-Couloume, G. Abiogenic formation of alkanes in the Earth's crust as a minor source for global hydrocarbon reservoirs. *Nature* **2002**, *416*, 522–524.
72. Lollar, B.S.; Lacrampe-Couloume, G.; Slater, G.F.; Ward, J.; Moser, D.P.; Gihring, T.M.; Lin, L.H.; Onstott, T.C. Unravelling abiogenic and biogenic sources of methane in the Earth's deep subsurface. *Chem. Geol.* **2006**, *226*, 328–339.
73. Taran, Y.A.; Giggenbach, W.F. Geochemistry of light hydrocarbons in subduction related volcanic and hydrothermal fluids. In *Volcanic, Geothermal, and Ore-Forming Fluids: Rulers and Witnesses of Processes within the Earth*; Simmons, S.F., Graham, I.J., Eds.; Special Publications of the Society of Economic Geologists. Littleton, CO, USA, 2003; pp. 61–74.
74. Etiope, G.; Lollar, B.S. Abiotic methane on Earth. *Rev. Geophys.* **2013**, *51*, 276–299.
75. Hoefs, J. *Stable Isotope in Geochemistry*, 5th ed.; Springer: Berlin, Germany, 2004; p. 244.
76. Jenden, P.D.; Drazan, D.J.; Kaplan, I.R. Mixing of Thermogenic Natural Gases in Northern Appalachian Basin. *AAPG Bull.* **1993**, *77*, 980–998.
77. Kawagucci, S.; Ueno, Y.; Takai, K.; Toki, T.; Ito, M.; Inoue, K.; Makabe, A.; Yoshida, N.; Muramatsu, Y.; Takahata, N.; et al. Geochemical origin of hydrothermal fluid methane in sediment-associated fields and its relevance to the geographical distribution of whole hydrothermal circulation. *Chem. Geol.* **2013**, *339*, 213–225.
78. Welhan, J.A.; Craig, H. Methane, hydrogen, and helium in hydrothermal fluids at 21°N on the East Pacific Rise. In *Hydrothermal Processes at Seafloor Spreading Centers*; Rona, P.A.; Bostrom, K., Laubier, L., Smith, K.L., Jr., Eds.; Plenum Press: New York, NY, USA, 1983; pp. 391–409.
79. Simoneit, B.R.T.; Lein, A.Y.; Peresypkin, V.I.; Osipov, G.A. Composition and origin of hydrothermal petroleum and associated lipids in the sulfide deposits of the Rainbow field (Mid-Atlantic Ridge at 36°N). *Geochim. Cosmochim. Acta* **2004**, *68*, 2275.
80. McCollom, T.M.; Seewald, J.S. Abiotic Synthesis of Organic Compounds in DeepSea Hydrothermal Environments. *Chem. Rev.* **2007**, *107*, 382–401.
81. Sano, Y.; Fischer, T.P. The Analysis and Interpretation of Noble Gases in Modern Hydrothermal Systems. In *The Noble Gases as Geochemical Tracers. Advances in Isotope Geochemistry*; Burnard, P., Ed.; Springer: Berlin/Heidelberg, Germany, 2013; pp. 249–317.

82. Giggenbach, W.; Sano, Y.; Wakita, H. Isotopic composition of helium, CO_2, and CH_4 contents in gases produced along the New Zealand part of a convergent plate boundary. Geochim. *Cosmochim. Acta* **1993**, *57*, 3427–3455.
83. Darling, W.G. Hydrothermal hydrocarbon gases: 1, genesis and geothermometry. *Appl. Geochem.* **1998**, *13*, 815–824.
84. Pfeiffer, L.; Bernard-Romeo, R.; Mazot, A.; Taran, Y.A.; Guevara, M.; Santoyo, E. Fluid geochemistry and soil gas fluxes (CO_2-CH_4-H_2S) at a promissory Hot dry Rock Geothermal System: The Acoculco caldera, Mexico. *J. Volcanol. Geoth. Res.* **2014**, *284*, 122–137.
85. Hilton, D.R.; Fischer, T.P.; Ballentine, C.J. *Noble Gases and Volatile Recycling at Subduction Zones*; Porcelli, D., Ballentine, C.J., Wieler, R., Eds.; Reviews in Mineralogy and Geochemistry 47; The Mineralogical Society of America: Washington, DC, USA, 2002; pp. 319–370.
86. Snyder, G.; Poreda, R.; Fehn, U.; Hunt, A. Sources of nitrogen and methane in Central American geothermal settings: Noble gas and ^{129}I evidence for crustal and magmatic volatile components. *Geochem. Geophy. Geosy.* 2003, *4*, 1–28.
87. Jenden, P.D.; Kaplan, I.R.; Poreda, R.J.; Craig, H. Origin of nitrogen-rich natural gases in the California Great Valley: Evidence from helium, carbon and nitrogen isotope ratios. *Geochim. Cosmochim. Acta* **1988**, *52*, 851–861.
88. Krooss, B.M.; Littke, R.; Müller, B.; Frielingsdorf, J.; Schwochau, K.; Idiz, E.F. Generation of nitrogen and methane from sedimentary organic matter: Implications on the dynamics of natural gas accumulations. *Chem. Geol.* **1995**, *126*, 291–318.
89. Marty, B.; Humbert, F. Nitrogen and argon isotopes in oceanic basalts. *Earth Planet. Sci. Lett.* **1997**, *152*, 101–112.
90. Zartman, R.E.; Reynolds, J.H.; Wasserburg, G.J. Helium, argon and carbon in some natural gases. *J. Geophys. Res.* **1961**, *66*, 277–306.
91. Matsuo, S.; Suzuki, M.; Mizutani, Y. Nitrogen to argon ratios in volcanic gases. In *Terrestrial Rare Gases*; Alexander, E.C., Jr., Ozima, M., Eds.; Center for Academic Publications: Japan, Tokyo, 1978; pp. 17–25.
92. Kiyosu, Y. Variations in N_2/Ar and He/Ar ratios of gases from some volcanic areas in Northeastern Japan. *Geochem. J.* **1986**, *19*, 275–281.
93. Sano, Y.; Pillinger, C.T. Nitrogen isotopes and N_2/Ar ratios in chests: An attempt to measure time evolution of atmospheric $\delta^{15}N$ value. *Geochem. J.* **1990**, *24*, 315–325.
94. Inguaggiato, S.; Taran, Y.; Grassa, F.; Capasso, G.; Favara, R.; Varley, N.; Faber, E. Nitrogen isotopes in thermal fluids of a forearc region (Jalisco Block, Mexico): Evidence for heavy nitrogen from continental crust. *Geochem. Geophys. Geosyst.* **2004**, *5*, Q12003. https://doi.org/10.1029/2004GC000767.
95. Zhang, L.; Zhang, Y.; Wang, A. Origins of N_2 in the Dongtai Depression of the Subei Basin. *Energy Explor. Exploit.* **2010**, *28*, 377–396.
96. Zhu, Y.; Shi, B.; Fang, C. The isotopic compositions of molecular nitrogen: Implications on their origins in natural gas accumulations. *Chem. Geol.* **2000**, *164*, 321–330.
97. Lyon, G.L.; Huiston, J.R. Carbon and hydrogen isotopic compositions of New Zealand geothermal gases. *Geochim. Cosmochim. Acta* **1984**, *48*, 1161–1171.
98. Bottinga, Y. Calculated fractionation factors for carbon and hydrogen isotope exchange in the system calcite-carbon dioxide-graphite-methane-hydrogen-water vapor. *Geochim. Cosmochim. Acta* **1969**, *33*, 49–64.
99. Arnorsson, S. *Isotopic and Chemical Techniques in Geothermal Exploration, Development and Use*; International Atomic Energy Agency, Vienna, 2000; p. 350.